Research Article Vol. 42, No. 5 / May 2025 / Journal of the Optical Society of America A B305

Journal of the Optical Society of America A

OPTICS, IMAGE SCIENCE, AND VISION

Importance of hue: the effect of saturation on hue–chroma asymmetries

Laysa Hedjar,[1,*] Matteo Toscani,[2] and Karl R. Gegenfurtner[1]

[1]Abteilung Allgemeine Psychologie, Justus-Liebig-Universität-Gießen, Gießen, Germany
[2]Department of Psychology, Bournemouth University, Poole BH12 5BB, UK
*laysa.hedjar@psychol.uni-giessen.de

Received 16 October 2024; revised 21 January 2025; accepted 4 February 2025; posted 5 February 2025; published 3 March 2025

Color spaces based on the cardinal color mechanisms, such as DKL, are not perceptually uniform: just-noticeable differences (JNDs) for chroma (and saturation) are larger than for hue, particularly in the orangish and less so in the purplish region. There is evidence that points of equal distance from the achromatic axis are not perceived as equally saturated, suggesting differential scaling between the quadrants. We measured hue and chroma JNDs as well as perceived saturation in the orangish and purplish quadrants of DKL. We calculated chroma-to-hue JND ratios as a function of perceived saturation and found that the ratios were still much higher in the orangish than the purplish quadrant.

https://doi.org/10.1364/JOSAA.544641

1. INTRODUCTION

Human color vision begins with the excitations of three photoreceptor types in the retina that respond to different parts of the visible spectrum: long-wavelength (L), middle-wavelength (M), and short-wavelength (S) sensitive types. Alone, a single photoreceptor type only signals increases or decreases in the intensity of the light to which it is sensitive. Subsequent neural stages of the visual pathway, however, compare the rates of photon absorption of the different types; these second-order mechanisms enable us to perceive color. Physiological evidence as well as computational work have identified three cardinal opponent mechanisms, $L+M$ (luminance), $L-M$, and $S-(L+M)$, which make up the dimensions of DKL color space [1–3].

DKL and similar physiologically based color spaces [4] are known to be nonuniform in terms of color perception; two color pairs equally spaced apart in the color space are not necessarily perceived as equally dissimilar [5]. This is true for suprathreshold color discrimination as well as discrimination at threshold. Particularly, discrimination thresholds measured along the radial directions of an isoluminant color plane, which signify changes in chroma (distance from the achromatic axis) or saturation (see Note [6]), tend to be larger than thresholds measured along the angular (or hue) directions [7–12]. This seems paradoxical given that the two isoluminant opponent mechanisms essentially signal chroma [7]. Danilova and Mollon, however, suggest that this "super-importance of hue" [5] might be attributed to correlated neural noise between individual channels. Since the two channels signal chroma differences, there is greater noise along the chroma dimension rather than the perpendicular hue dimension. Regan *et al.* [13], using an adaptation paradigm, did not find support for separate neural channels for hue and saturation but do suggest that more than one mechanism is used to detect such changes.

The "correlated neural noise" hypothesis, however, does not explain the fact that the relationship between hue and chroma thresholds across post-receptoral color spaces is not consistent. In the positive $L-M$, negative $S-LM$ quadrant 4 (roughly, orangish [14] colors) and the negative $L-M$, positive $S-LM$ quadrant 2 (roughly, bluish colors) of DKL, hue discrimination thresholds are significantly smaller than chroma. For colors in the other two quadrants (roughly, purplish and greenish), hue thresholds are almost as large as chroma thresholds [7–12]. Currently, it is unclear whether this disparity arises from the distribution of colors in our environment. Physiological data from V2 and beyond show regions narrowly tuned to a variety of hues around the color circle [15,16]. Particularly, magnetoencephalography (MEG) results from Rosenthal *et al.* have shown more discriminable hue tuning for warmer colors [17,18], which also coincides with object colors and is also reflected by the more varied terms we have for them [19,20]. Lastly, deep neural networks trained on object recognition using the ImageNet database have more kernels, i.e., the equivalent of "receptive fields" in biological sensory systems, which are particularly sensitive to bluish and orangish hues more so than other colors [21,22]. These studies support the notion that our visual system has evolved better hue discrimination for certain colors due to the environment, but the relationship between hue and chroma discrimination is not explicitly explored.

Here, we consider that the disparity in thresholds across DKL color space is due to differences in the perception of saturation. Figure 1 plots points of subjective equality for saturation in DKL color space, derived from data collected in

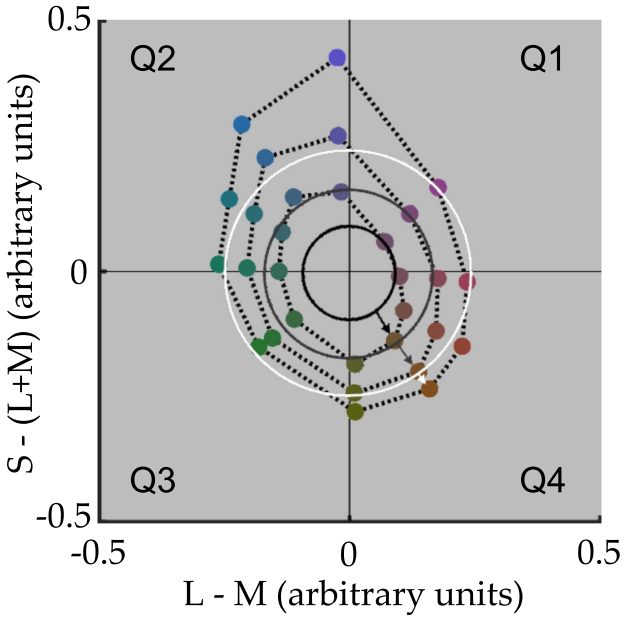

Fig. 1. Points of subjective equality (PSEs) for saturation on an equiluminant plane in DKL color space. Dotted lines connect points that are perceived to have equal saturation. For comparison, solid rings anchored at the points bisecting the first quadrant (purplish) illustrate points which have equal values of saturation and chroma as defined [6]. The dotted lines and circles do not overlap, indicating that this definition of saturation does not represent the percept of saturation very well. The shift needed for points in the fourth quadrant (orangish) to be perceived as equally saturated as those in the first is denoted with arrows. Derived from data published in Schiller *et al.* [23].

CIELAB space by Schiller *et al.* [23]. The dotted lines connect colors that observers judged to be equally saturated. The solid rings denote colors with equal chroma and equal saturation values as formally defined [6]. One can see that the ellipses connecting the points of subjective equality are tilted along the negative diagonal—that is, elongated toward the bluish and orangish quadrants. Thus, colors in the orangish quadrant must be increased in chroma in order to be perceived as equally saturated as colors in the purplish quadrant. This means that, at equal chromas, Q1 colors are perceived as more saturated than Q4.

Discrimination thresholds are typically smallest for colors closest to the adaptation point [11]. Along the cardinal directions, chroma thresholds increase linearly as one moves away from the adaptation point, while hue thresholds—along the orthogonal cardinal directions—stay constant [11]. It is possible that hue and chroma thresholds scale differently in the diagonal directions—e.g., as one increases chroma, hue thresholds may increase at a slower rate in the orangish quadrant compared to the purplish, while the rate of chroma thresholds increases more comparably. The aim of this experiment was to determine if the differences in discrimination thresholds between quadrants could be eliminated if we equated perceived saturation between quadrants. We measured points of subjective equality (PSEs) for saturation at three chroma radii and then measured chroma and hue discrimination thresholds at those same three chroma radii for the purplish (Q1) and orangish (Q4) quadrants in DKL space. We scaled the chroma radii for the two quadrants based on the saturation PSEs and then compared chroma-to-hue threshold ratios between the quadrants. We found that the chroma-to-hue threshold ratio was still significantly larger in the orangish quadrant compared to the purplish quadrant even when equating perceived saturation. Generally, there was a significant but modest effect of saturation on chroma-to-hue threshold ratios in both orangish and purplish quadrants.

2. METHODS

A. Definition of DKL Color Space

We used the conventions explained by Hansen and Gegenfurtner [24] to define the axes of DKL. The center of the isoluminant plane was the monitor at midgray (CIE1931 Judd-corrected $xyY = 0.311,\ 0.328,\ 60.8$). The xyY coordinates of the RGB channels, measured with a Konica Minolta CS2000A spectroradiometer, were R = (0.6865, 0.3107, 30.4517), G = (0.2105, 0.7279, 83.9947), and B = (0.1502, 0.0451, 7.1184). The DKL-to-RGB transformation matrix was as shown in Table 1. These were calculated using Smith and Pokorny's [25] 2° fundamentals with Boynton's [26] Z coefficient value.

The scaling of the chromatic axes of DKL is not standardized [27], so we chose to scale the S axis such that the average detection thresholds around the adaptation point were approximately circular [9–12,28,29]. We expect that deviations from the separability of the L − M and S − (L + M) mechanisms are largest when both mechanisms are activated equally, which is the case when both are equally above the threshold. Five experienced observers, including one of the authors, performed a detection task: a 0.5° diameter disc could appear in one of the four locations around the fixation point at the center of the screen. The four possible disc locations were arranged in a square with 0.5° horizontal and vertical spacing between disc edges. We measured detection thresholds in eight hue directions from the adaptation point, although we only used thresholds along the cardinal axes to define the scaling factor. The disc differed in chroma from the adaptation point in predefined steps. The number of steps predefined for each hue angle and the distance of the maximum step varied across participants, ranging from 15 steps between 0 and 0.1 units to 29 steps between 0 and 0.14 units. The chroma shift of the disc was determined with a QUEST adaptive staircase [30] for each hue direction; trials across hues were interleaved. The disc appeared on the screen for 500 ms, after which observers could indicate its location using the keyboard. They received feedback on their performance (click sound = correct, white noise sound = incorrect). Sixty-five trials were collected for each staircase except for one observer (an author), for whom 60 trials were collected. The observers completed the task in two blocks, about 13 min each. We used the *psignifit* toolbox [31] to fit psychometric curves to the data, with a lower limit at 25% correct. Detection thresholds

Table 1. DKL-to-RGB Transformation Matrix

	L + M	L − M	S − (L + M)
R	1	1	0.0868
G	1	−0.3641	−0.1162
B	1	0.0182	1

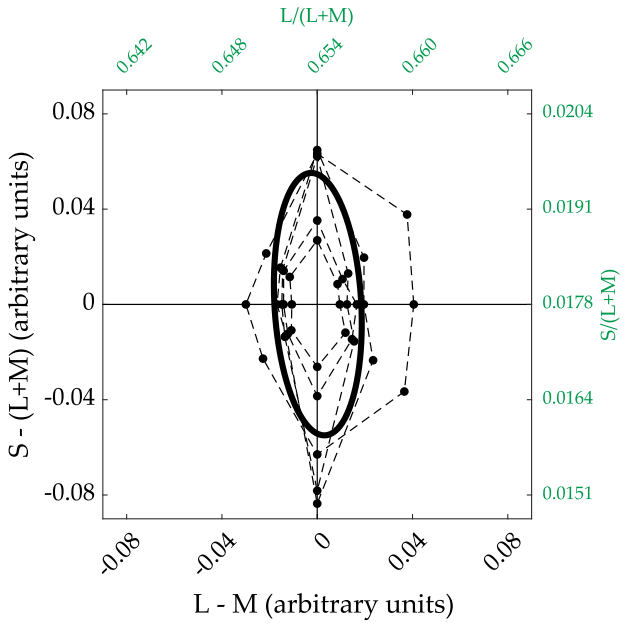

Fig. 2. Chroma detection thresholds at the adaptation point (0,0). Individual detection thresholds are plotted as black dots and connected with thin dashed lines. We fit an ellipse to the thresholds averaged across observers (thick line). The x and y axis are defined in detection threshold units. We also include MacLeod–Boynton coordinates [4] for reference.

were defined at 62.5% correct. Figure 2 shows the resulting thresholds for the five participants as well as a best-fit line. To compute the S axis scaling factor, we averaged the thresholds along the L − M axis (1 L − M detection threshold unit) and along the S axis (1 S − (L + M) detection threshold unit) across participants. We divided the S axis threshold mean by the L − M axis threshold mean to get a factor of 2.93. All DKL coordinates and distances from here on are defined in this scaled space, with axes plotted in detection threshold units.

Note that the fitted black ellipse is closely aligned with the axes and has a very slight tilt towards the negative diagonal, similar to those found in other studies [9,10,12]. However, the tilt is considerably smaller than in Bosten *et al.*'s discrimination ellipses at the adaptation point [32]. A key difference between our study and theirs is that Bosten *et al.* used a luminance pedestal of >38% contrast for their stimuli.

All stimuli were presented on an Eizo ColorEdge CG2420 (10 bits/channel) monitor with a resolution of 1920 × 1200 (49.25° × 32°). We used Psychtoolbox 3 on MATLAB R2019b to present the stimuli, which were gamma-corrected before presentation. Observers sat 56.5 cm away from the screen.

B. Stimuli and Procedure

For the measurement of both discrimination thresholds and saturation PSEs, reference points for Quadrant 1 (Q1: purplish) and Quadrant 4 (Q4: orangish) bisected the quadrants at approximately 3.2, 6.5, and 9.2 detection threshold units away from the origin. Table 2 notes the xyY values of the six reference colors, and Fig. 3(a) shows the isoluminant plane with the reference points and the hue and chroma directions.

Table 2. *xyY* Values of Reference Colors

	x	y	Y
Q1, radius 3.2	0.3065	0.2936	60.79
Q1, radius 6.5	0.3031	0.2659	60.74
Q1, radius 9.2	0.3008	0.2468	60.79
Q4, radius 3.2	0.3361	0.3594	60.75
Q4, radius 6.5	0.3669	0.3982	60.74
Q4, radius 9.2	0.3981	0.4377	60.81

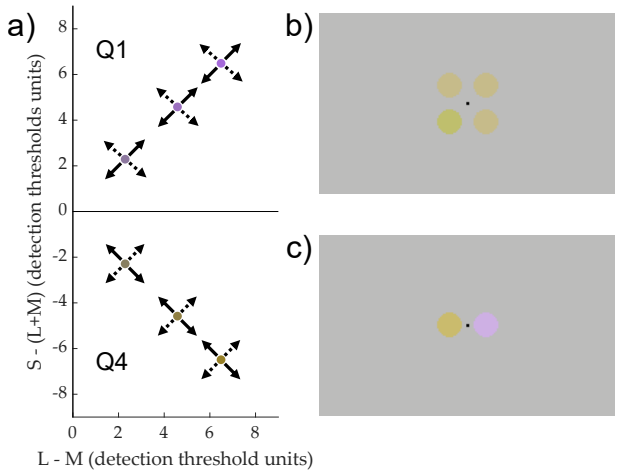

Fig. 3. (a) Reference stimuli (colored dots) and directions tested for discrimination experiment or point of subjective equality (PSE) experiment in DKL (scaled). For the discrimination experiment, three discs were fixed at the reference color while one odd-one-out was shifted in either chroma (solid arrows) or hue (dashed arrows). For the saturation PSE experiment, one disc was fixed at one reference color while the other varied in chroma (solid arrows) in the opposite quadrant. The shifts were determined by an adaptive staircase based on the observer's previous responses. (b, c) Sample stimulus from the discrimination experiment (b) and the saturation PSE experiment (c) (enlarged for visibility).

1. Discrimination Thresholds

We measured hue and chroma discrimination thresholds at the six Q1 and Q4 reference points. Four 0.5° diameter discs were presented in a square arrangement with the horizontal and vertical distance between disc edges at 0.5°, similar to Krauskopf and Gegenfurtner [11]. We show a sample stimulus in Fig. 3(b). Three of the four discs had the color of the reference, while the color of one was shifted in either hue (clockwise or counterclockwise along the tangent) or chroma (positive or negative) 0 to 10 steps away from the reference. The magnitudes of the color shifts were chosen such that they encompassed the dynamic range of observers' thresholds. Figure 3(a) shows the possible color shift directions for each reference color. The maximum shift possible was 1.87 detection threshold units from the reference. The color shift of the odd disc presented on each trial was determined by the adaptive staircase method QUEST [30]. We collected 70 trials per condition [two quadrants × three chroma radii × four directions (cw and ccw hue, positive and negative chroma)].

Each stimulus set was presented for 500 ms; after the presentation, observers used the keyboard to indicate which of the

four discs was the "odd-one-out." They were told to focus on differences in color, not shape or size. The intertrial interval was 1000 ms, during which observers were given auditory feedback on their performance (click sound = correct; white noise = incorrect). Trials were blocked by the chroma radius of the reference; all other conditions were interleaved. Each block began with 20 practice trials. To help observers grow accustomed to the task and the stimuli, the presentation time was 2000 ms for the first eight practice trials, 1000 ms for the next four, and 500 ms for the last eight. The practice trials merged seamlessly with the experimental trials.

2. Saturation PSEs

We wanted to calculate the chroma needed for an orangish disc to appear as equally saturated as a purplish disc of a fixed chroma (and vice versa). Observers were presented with two uniform discs and asked to choose which appeared more saturated. The color of one disc was fixed at the reference point for one of the quadrants, while the other (test) disc came from the other quadrant [Fig. 3(c)]. The chroma of the test disc was determined using an adaptive staircase similar to QUEST. The staircase started with a normal distribution prior centered on the chroma of the reference. With each response, the prior was updated, and the chroma for the next trial was chosen from the weighted prior. Figure 3(a) indicates the increasing and decreasing chroma directions for each reference point (solid arrows). There were 11 possible chroma steps ranging from 0 units from the reference to 1.87 detection threshold units. We collected 70 trials per condition (two quadrants × three chroma radii).

Each disc had a diameter of 0.5° and the horizontal spacing between disc edges was 0.5°. The positions (left or right) of the reference and the test discs were randomized. Each stimulus pair was presented at the center of the screen for 500 ms; after the presentation, observers indicated using a keyboard which disc appeared more saturated. The intertrial interval was 1000 ms. Trials were blocked by the chroma radius of the reference; the blocks were completed in random order with a self-paced break halfway. Each block began with 20 practice trials in order for observers to grow accustomed to the task: for the first eight trials, the presentation time was 2000 ms; for the next four, 1000 ms, and for the last eight, 500 ms. The practice trials merged seamlessly with the experimental trials. On the instructions screen, we presented a green pepper at four levels of increasing saturation to help orient observers toward the definition of saturation.

C. Participants

Sixteen naïve observers (13 female) completed the tasks. Observers' ages ranged from 19 to 56 years old with a mean age of 26.9 years. All observers gave informed consent and had normal color vision as assessed by the Ishihara Color Vision Test [33].

D. Analyses

For all statistical analyses, we fitted linear mixed-effects models (LMMs) using the *nlme* package [34] in the R programming environment [35]. All LMMs were fitted using the restricted maximum-likelihood method. We ran ANOVAs and *t*-tests using the built-in R package stats. All *post hoc* contrasts were performed using the *emmeans* package [36] with Bonferroni-corrected *p*-values.

3. RESULTS

A. Discrimination Thresholds

We fitted psychometric curves to each observer's data using the *psignifit* toolbox [31]. We defined the lower limit at 25% correct (chance level for 4AFC) and the upper limit at 100% correct, so discrimination thresholds were defined at 62.5% correct. Figure 4 plots individual and mean JNDs across participants. We can see on the right that thresholds in the orangish quadrant are more elliptical than thresholds in the purplish quadrant. For statistical testing, thresholds were averaged between directions (i.e., between positive and negative chroma, and between cw and ccw hue), but we note that decreasing chroma thresholds were significantly larger than increasing for all pairs except orangish at radius = 9.2 ($p < 0.01$). We found that the linear mixed-effects model best fit to our data [determined by comparing Akaike information criterion (AIC)] used *color dimension*, *quadrant*, and *reference chroma* as fixed-effects factors with interactions specified between *quadrant* and *color dimension* as well as *quadrant* and *radius*. We set *observer* as a random-effects factor with slopes varying according to *radius*. To meet model assumptions, we used *log JND* as the dependent variable. We applied a three-way ANOVA to this model. Figure 4 (left) illustrates the main effects: chroma JNDs (open circles) were greater than hue JNDs [filled circles; $F(1, 361) = 132.5$, $p < 0.001$], and purplish JNDs were larger than orangish JNDs [$F(1, 361) = 153.8$, $p < 0.001$]. There was also a significant difference between radii [$F(2, 361) = 51.4$, $p < 0.001$]. Pairwise contrasts with Bonferroni corrections indicated that JNDs at radius 9.2 were greater than at 6.5, which were greater than at 3.2 [9.2 versus 6.5: $t(361) = 4.78$; 6.5 versus 3.2: $t(361) = 7.36$; 9.2 versus 3.2: $t(361) = 10.1$; $p < 0.001$ for all tests].

There was a significant interaction between *quadrant* and *color dimension* [$F(1, 361) = 76.2$, $p < 0.001$]: orangish hue thresholds were significantly smaller than orangish chroma as well as purplish hue and chroma thresholds ($p < 0.001$ for all tests). However, despite a significant main effect of *color dimension*, purplish hue thresholds were not significantly smaller than purplish chroma [$F(1, 361) = 1.97$, $p = 0.3$]. An interaction between *quadrant* and *radius* was also found [$F(2, 361) = 6.72$; $p = 0.001$]. All contrasts were significant ($p \leq 0.008$) except between orangish thresholds at a radius of 6.5 and purplish thresholds at 3.2 [$t(361) = 1.16$, $p = 1.0$] and orangish at 9.2 [$t(361) = 2.95$, $p = 0.05$]. In particular, purplish thresholds at 6.5 were larger than orangish at 9.2 [$t(361) = 4.21$, $p < 0.001$] and 6.5 [$t(361) = 7.83$, $p < 0.001$].

B. Saturation PSEs

Responses were quantified as the percentage of trials per chroma step at which the observers chose the reference as more saturated. We fitted psychometric curves to this data using the

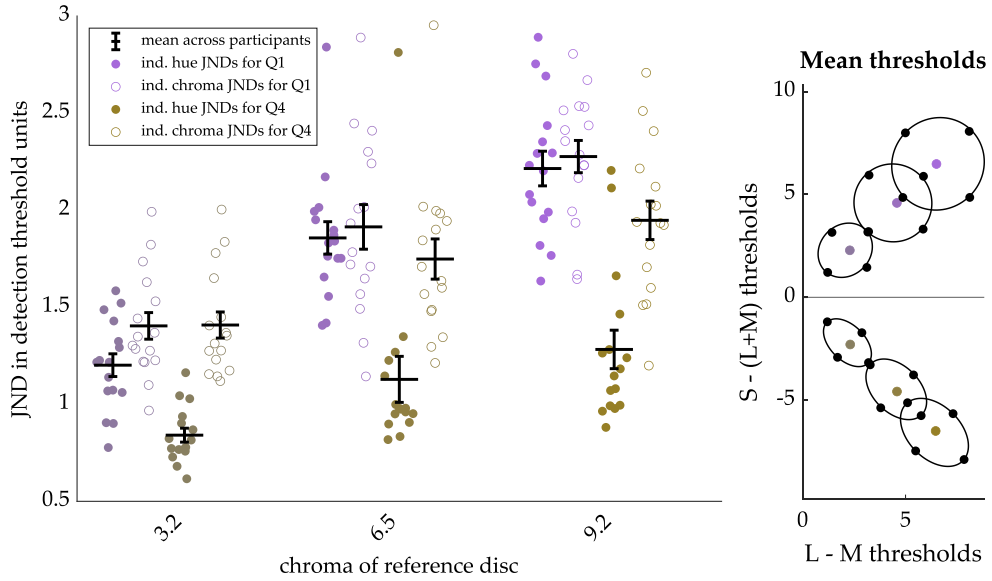

Fig. 4. Hue and chroma JNDs across participants for Q1 and Q4 at the three chromas tested. (Left) Data are separated by chroma radius on the x axis. Individual JNDs, averaged between directions, are plotted with colored circles (either purplish for Q1 or orangish for Q4). Data are jittered along the x axis for visibility. Filled circles represent hue JNDs and open circles chroma JNDs. Means across participants are plotted as black lines; error bars represent ± 1 SEM. (Right) Mean thresholds are plotted in DKL space as black dots. Reference colors are plotted as purplish for Q1 and orangish for Q4. Ellipses are fitted around the thresholds surrounding each reference color. Chroma thresholds fall along the radial lines from the origin, and hue thresholds fall along tangents to hue circles passing through the reference. See text for significance tests.

psignifit toolbox for MATLAB [31]. The lower and upper limits of the function were 0% (never chose the reference as more saturated) and 100% (always chose the reference as more saturated), so PSEs were defined at 50%.

Figure 5 plots the chroma values of the test disk for each reference point. An orange dot represents the Q4 chroma value perceived as equally saturated as the fixed Q1 reference (plotted as a thick purple line), and vice versa, for an individual observer. The means across participants are plotted as black lines with error bars representing ± 1 SEM. On average, chroma values of the orangish test disk must be larger than those of the purplish reference disk in order to be perceived as equally saturated. Conversely, one must reduce the chroma of a purplish test disk in order for it to be perceived as equally saturated as an orangish disc. Together these imply that, at equal chromas, Q1 (purplish) discs are perceived as more saturated than Q4 (orangish) discs, although the difference is slight.

We first compared PSE chroma shifts against the reference chroma for each condition. We performed six one-sample t-tests (Bonferroni-corrected p-values) comparing the difference in chroma PSEs of the test disk and the reference chroma against 0. Only two of the six tests were significant: observers increased the chroma of orangish discs to match the saturation PSE of the chroma 3.2 purplish reference [$t(15) = 2.98$, $p = 0.047$], and decreased the chroma of purplish discs to match the saturation of the chroma 3.2 orangish reference [$t(15) = 3.39$, $p = 0.024$]. The other four tests were non-significant ($p > 0.17$).

In order to compare chroma-to-hue ratios of the two quadrants at equal perceived saturation, we scaled the Q4 chroma axis such that equal chroma radii from Q1 and Q4 have the same perceived saturation. For each individual observer, we calculated scaling factors based on the PSEs of each of the six conditions (three chroma radii from two quadrants). For each condition, scaling factors were calculated by dividing the mean chroma

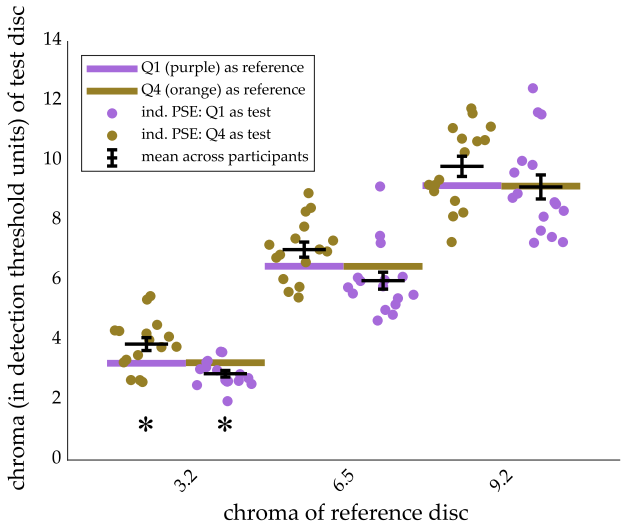

Fig. 5. Individual saturation PSEs for Q1 and Q4 at each chroma radius. Results are grouped by the chroma radius of the reference (x axis), with Q1 (purplish) as the reference on the left and Q4 (orangish) as the reference on the right of each group. On the y axis, we plot the chroma value of the test disk at which observers perceived the test and reference disk of equal saturation (PSE). Orange dots represent chroma values of the test disk when the reference was Q1, and vice versa. Individual observer values are jittered along the x axis for visibility. For comparison, the chroma value of the reference is plotted as a thick colored line. The mean across participants is plotted as a black line with error bars representing ± 1 SEM. Results of one-sample t-tests against the reference chroma for each condition are represented by asterisks: $^{*}p < 0.05$, $^{**}p < 0.001$, and $^{***}p < 0.001$.

PSEs by the chroma of the reference disc. We then computed the geometric mean of the scaling factors for a given observer.

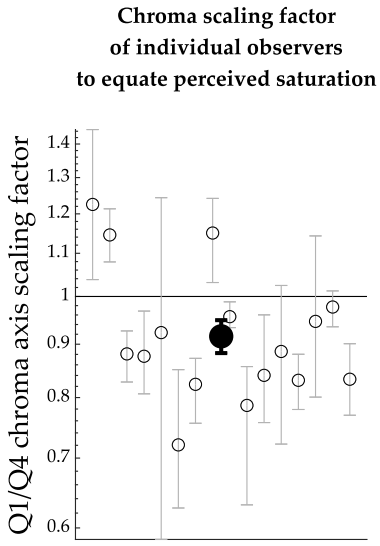

Fig. 6. Individual Q1/Q4 reference chroma scaling factors. Open black circles are individual average scaling factors, with bars indicating the range of scaling factors from the six conditions. The filled black dot is the average scaling factor across participants, with ±1 SEM error bars [37]. The y axis is plotted on a log scale. A scaling factor of less than 1 means observers needed to reduce Q1 chroma values in order to equate perceived saturation with Q4.

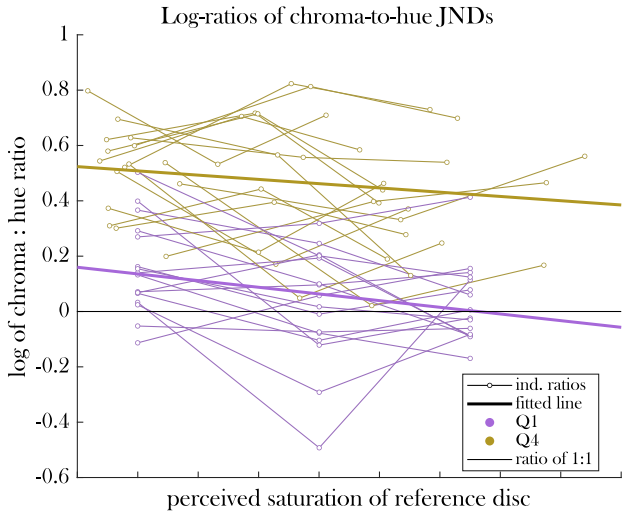

Fig. 7. Log ratio of chroma:hue thresholds per quadrant. Chroma of the reference color increases from left to right along the x axis but is scaled per quadrant such that at a given x value, perceived saturation between quadrants is equal [using individual Q4 scaling factors from each participant (Fig. 6); see text for details]. The y axis plots the log of the ratio of chroma to hue JNDs, color-coded according to quadrant. Open circles connected by thin lines represent individual observer ratios. Thick lines are fitted across individuals.

Across observers, the average Q4 chroma axis scaling factor was 0.91; the Q4 orangish reference chromas we measured are perceived as less saturated than the Q1 purplish reference chromas, so the Q4 chroma axis scaling factor is less than 1. Figure 6 plots the average Q4 chroma scaling factors for each individual observer as well as the group average. A one-sample t-test against 1 indicates that the factors are significantly different from 1 [$t(15) = -2.13$, $p = 0.0497$].

In Fig. 7, we plot the log ratios of chroma-to-hue JNDs for each quadrant; perceived saturation (scaled chroma) is plotted on the x axis, using individual scaling factors obtained from each observer. The three observers whose scaling factors were larger than 1 (i.e., who perceived Q4 chromas as more saturated than Q1) have their Q4 chroma-to-hue ratios shifted to the right of the Q1 ratios. We applied an ANCOVA on the log of the chroma-to-hue ratios with *quadrant* as a main factor, *scaled chroma* as a covariate, and *observer* as a random effect. We found a main effect of *quadrant* [$F(1, 78) = 143.7$, $p < 0.001$], where chroma-to-hue ratios in Q1 were higher than in Q4. *Scaled chroma* had a significant linear relationship with chroma-to-hue ratio [$F(1, 78) = 8.36$, $p = 0.005$; model coefficient = −1.10]—the smaller the scaled chroma value, the larger the chroma-to-hue ratio. It is clear from Fig. 7 that, even with perceived saturation equated between quadrants, the chroma-to-hue ratio is still lower in the purplish quadrant than the orangish across all saturation levels. Although the effect of *scaled chroma* was significant, the ratios for both quadrants are nearly constant across chroma radii; therefore, even a larger difference in perceived saturation (i.e., a larger scaling factor) would have little effect on closing the disparity between quadrants.

4. DISCUSSION

We examined whether the nonuniformity of thresholds in DKL space can be explained by differences in perceived saturation. Specifically, we explored differences in hue and chroma thresholds between colors in the orangish (+[L − M] and −[S − [L + M]]) and purplish (+[L − M] and +[S − [L + M]]) quadrants. Previous work has shown that hue JNDs in the orangish quadrant are much smaller than chroma JNDs, whereas in the purplish quadrant, they are approximately equal [7–12]. We found that accounting for differences in perceived saturation did not eliminate this disparity.

First, we measured hue and chroma JNDs at three chroma radii. The chroma:hue ratio was higher in the orangish than the purplish quadrant, supporting previous literature [7–12]. Then, we measured points of subjective equality (PSEs) for saturation at the same three chroma radii and found that orangish stimuli were perceived to be slightly less saturated than purplish stimuli (Fig. 5; see also Fig. 1). However, this difference was relatively small—on average a chroma shift of less than half of a chroma JND—and was significantly different only for the reference colors with the smallest chroma radius. Plotting the chroma:hue ratios as a function of perceived saturation, we can see clearly in Fig. 7 that chroma and hue thresholds are approximately equal for purplish colors (roughly 10:9) while for orangish colors, hue thresholds are much smaller than chroma thresholds (roughly 10:6).

Figure 7 shows that on average there is a slight decrease in the chroma:hue JND ratio as one increases perceived saturation, but that the slopes are relatively flat and similar between quadrants, indicating that hue and chroma thresholds increase at the same rate according to Weber's law. This also means that perceived saturation differences would have to be very large in order for the

ratios between quadrants to overlap. Given that we found only modest differences between chroma and perceived saturation, we find this is unlikely.

We also found that raw thresholds in general were higher in the purplish than the orangish quadrant, corroborating earlier research [9,10,12]. This means that the difference in threshold ratios between quadrants is driven not just by hue discrimination but chroma discrimination as well. Given this, neural noise along the chroma dimension [7] could only account for some of the threshold increases for chroma unless we consider higher-order mechanisms [9,24,38]. We know from physiological work that cortical color preferences beyond V1 are much less aligned with the cardinal color directions [15,16,18,39–44], so restructuring of these mechanisms must occur in the stages following processing in the LGN at the earliest. Efforts at understanding these pathways are still ongoing and extensive.

We also know from previous work that many factors can influence discrimination performance, such as the adaptation point used [9,10,45,46], the background surrounding the stimulus as well as the variation of the stimulus and/or background [9,10,32,47–51], and the natural statistics of the environment [52,53], which were not explicitly tested here.

5. CONCLUSION

The importance of hue in the orangish quadrant of DKL space is particularly profound: discrimination thresholds for hue are much smaller than chroma thresholds. However, in the purplish quadrant, they are nearly equal. We considered whether differences in perceived saturation could account for this disparity. We found that perceived saturation showed minimal deviation from chroma and saturation as defined, and that differences in the chroma-to-hue threshold ratio between quadrants remained even after adjusting for it.

Funding. European Research Council (Advanced Grant Color 3.0 (884116)).

Acknowledgment. The authors would like to thank Fenja Hornung for helping with data collection.

Disclosures. The authors declare no conflicts of interest.

Data availability. Data underlying the results presented in this paper are available in Ref. [54].

REFERENCES AND NOTES

1. R. L. De Valois, I. Abramov, and G. H. Jacobs, "Analysis of response patterns of LGN cells*," J. Opt. Soc. Am. **56**, 966–977 (1966).
2. A. M. Derrington, J. Krauskopf, and P. Lennie, "Chromatic mechanisms in lateral geniculate nucleus of macaque," J. Physiol. **357**, 241–265 (1984).
3. J. Krauskopf, D. R. Williams, and D. W. Heeley, "Cardinal directions of color space," Vis. Res. **22**, 1123–1131 (1982).
4. D. I. MacLeod and R. M. Boynton, "Chromaticity diagram showing cone excitation by stimuli of equal luminance," J. Opt. Soc. Am. **69**, 1183–1186 (1979).
5. D. B. Judd, "Ideal color space redefined," Palette **31**, 23–29 (1969).
6. Saturation is usually defined as chroma related to lightness. When lightness is constant, such as in the MacLeod-Boynton chromaticity diagram or a plane of constant luminance in DKL space, the two measures become equivalent.
7. M. V. Danilova and J. D. Mollon, "Superior discrimination for hue than for saturation and an explanation in terms of correlated neural noise," Proc. Biol. Sci. **283**, 20160164 (2016).
8. M. V. Danilova and J. D. Mollon, "Symmetries and asymmetries in chromatic discrimination," J. Opt. Soc. Am. A **31**, A247–A253 (2014).
9. M. Giesel, T. Hansen, and K. R. Gegenfurtner, "The discrimination of chromatic textures," J. Vis. **9**(9):11, 11 (2009).
10. T. Hansen, M. Giesel, and K. R. Gegenfurtner, "Chromatic discrimination of natural objects," J. Vis. **8**(1):2, 1–19 (2008).
11. J. Krauskopf and K. Gegenfurtner, "Color discrimination and adaptation," Vis. Res. **32**, 2165–2175 (1992).
12. L. Hedjar, M. Toscani, and K. R. Gegenfurtner, "Importance of hue: color discrimination of three-dimensional objects and two-dimensional discs," J. Opt. Soc. Am. A **42**, B296–B304 (2025).
13. S. E. Regan, R. J. Lee, D. I. A. MacLeod, *et al.*, "Are hue and saturation carried in different neural channels?" J. Opt. Soc. Am. A **35**, B299–B308 (2018).
14. We use "purplish," "bluish," "greenish," and "orangish" to describe the colors in quadrants 1, 2, 3, and 4 of DKL color space because they roughly represent their appearance. Observers may actually use different terms.
15. K. S. Bohon, K. L. Hermann, T. Hansen, *et al.*, "Representation of perceptual color space in macaque posterior inferior temporal cortex (the V4 complex)," eNeuro **3**, ENEURO.0039-16.2016 (2016).
16. D. C. Kiper, S. B. Fenstemaker, and K. R. Gegenfurtner, "Chromatic properties of neurons in macaque area V2," Visual Neurosci. **14**, 1061–1072 (1997).
17. I. A. Rosenthal, S. R. Singh, K. L. Hermann, *et al.*, "Color space geometry uncovered with magnetoencephalography," Current Biol. **31**, 515–526.e5 (2021).
18. I. A. Rosenthal, S. Ratnasingam, T. Haile, *et al.*, "Color statistics of objects, and color tuning of object cortex in macaque monkey," J. Vis. **18**(11):1, 1 (2018).
19. B. R. Conway, S. Ratnasingam, J. Jara-Ettinger, *et al.*, "Communication efficiency of color naming across languages provides a new framework for the evolution of color terms," Cognition **195**, 104086 (2020).
20. E. Gibson, R. Futrell, J. Jara-Ettinger, *et al.*, "Color naming across languages reflects color use," Proc. Natl. Acad. Sci. USA **114**, 10785–10790 (2017).
21. A. Flachot and K. R. Gegenfurtner, "Color for object recognition: hue and chroma sensitivity in the deep features of convolutional neural networks," Vis. Res. **182**, 89–100 (2021).
22. A. Flachot and K. R. Gegenfurtner, "Processing of chromatic information in a deep convolutional neural network," J. Opt. Soc. Am. A **35**, B334 (2018).
23. F. Schiller, M. Valsecchi, and K. R. Gegenfurtner, "An evaluation of different measures of color saturation," Vis. Res. **151**, 117–134 (2018).
24. T. Hansen and K. R. Gegenfurtner, "Higher order color mechanisms: evidence from noise-masking experiments in cone contrast space," J. Vis. **13** (1):26, 26 (2013).
25. V. C. Smith and J. Pokorny, "Spectral sensitivity of the foveal cone photopigments between 400 and 500 nm," Vis. Res. **15**, 161–171 (1975).
26. R. M. Boynton, *Human Color Vision* (Holt, Rinehart & Winston, 1979).
27. R. L. De Valois, K. K. De Valois, and L. E. Mahon, "Contribution of S opponent cells to color appearance," Proc. Natl. Acad. Sci. USA **97**, 512–517 (2000).
28. Q. Zaidi and A. G. Shapiro, "Adaptive orthogonalization of opponent-color signals," Biol. Cybern. **69**, 415–428 (1993).
29. A. J. Vingrys and L. E. Mahon, "Color and luminance detection and discrimination asymmetries and interactions," Vis. Res. **38**, 1085–1095 (1998).
30. A. B. Watson and D. G. Pelli, "Quest: a Bayesian adaptive psychometric method," Percept. Psychophys. **33**, 113–120 (1983).
31. H. H. Schütt, S. Harmeling, J. H. Macke, *et al.*, "Painfree and accurate Bayesian estimation of psychometric functions for (potentially) overdispersed data," Vis. Res. **122**, 105–123 (2016).
32. J. M. Bosten, R. D. Beer, and D. I. A. MacLeod, "What is white?" J. Vis. **15**(16):5, 5 (2015).

33. S. Ishihara, *Ishihara's Tests for Colour Deficiency*, 38th ed. (Kanehara and Co., Ltd., 2018).
34. J. Pinheiro, D. Bates, and R. C. Team, "Nlme: linear and nonlinear mixed effects models" (2023).
35. R. C. Team, *R: a Language and Environment for Statistical Computing* (R Foundation for Statistical Computing, 2023).
36. R. V. Lenth, "Emmeans: estimated marginal means, aka least-squares means," (2023).
37. N. Norris, "The standard errors of the geometric and harmonic means and their application to index numbers," Ann. Math. Stat. **11**, 445–448 (1940).
38. J. Krauskopf, D. R. Williams, M. B. Mandler, *et al.*, "Higher order color mechanisms," Vis. Res. **26**, 23–32 (1986).
39. B. R. Conway and D. Y. Tsao, "Color-tuned neurons are spatially clustered according to color preference within alert macaque posterior inferior temporal cortex," Proc. Natl. Acad. Sci. USA **106**, 18034–18039 (2009).
40. B. R. Conway, S. Moeller, and D. Y. Tsao, "Specialized color modules in macaque extrastriate cortex," Neuron **56**, 560–573 (2007).
41. K. Koida and H. Komatsu, "Effects of task demands on the responses of color-selective neurons in the inferior temporal cortex," Nat. Neurosci. **10**, 108–116 (2007).
42. H. Komatsu, Y. Ideura, S. Kaji, *et al.*, "Color selectivity of neurons in the inferior temporal cortex of the awake macaque monkey," J. Neurosci. **12**, 408–424 (1992).
43. R. Lafer-Sousa, Y. O. Liu, L. Lafer-Sousa, *et al.*, "Color tuning in alert macaque V1 assessed with fMRI and single-unit recording shows a bias toward daylight colors," J. Opt. Soc. Am. A **29**, 657 (2012).
44. P. Lennie, J. Krauskopf, and G. Sclar, "Chromatic mechanisms in striate cortex of macaque," J. Neurosci. **10**, 649–669 (1990).
45. D. Cao and Y. H. Lu, "Chromatic discrimination: differential contributions from two adapting fields," J. Opt. Soc. Am. A **29**, A1–A9 (2012).
46. Q. Zaidi, B. Spehar, and J. DeBonet, "Adaptation to textured chromatic fields," J. Opt. Soc. Am. A **15**, 23–32 (1998).
47. N. Goda and M. Fujii, "Sensitivity to modulation of color distribution in multicolored textures," Vis. Res. **41**, 2475–2485 (2001).
48. M. Jansen, M. Giesel, and Q. Zaidi, "Segregating animals in naturalistic surroundings: interaction of color distributions and mechanisms," J. Opt. Soc. Am. A **33**, A273–A282 (2016).
49. A. Li and P. Lennie, "Mechanisms underlying segmentation of colored textures," Vis. Res. **37**, 83–97 (1997).
50. S. F. Pas and J. J. Koenderink, "Visual discrimination of spectral distributions," Perception **33**, 1483–1497 (2004).
51. V. Singh, J. Burge, and D. H. Brainard, "Equivalent noise characterization of human lightness constancy," J. Vis. **22**(5):2, 2 (2022).
52. A. E. Skelton, A. Franklin, and J. M. Bosten, "Colour vision is aligned with natural scene statistics at 4 months of age," Dev. Sci. **26**, e13402 (2023).
53. A. E. Skelton, J. Maule, S. Floyd, *et al.*, "Effects of visual diet on colour discrimination and preference," Proc. Biol. Sci. **291**, 20240909 (2024).
54. L. Hedjar, M. Toscani, and K. R. Gegenfurtner, "Dataset: Importance of hue: the effect of saturation on hue–chroma asymmetries," Zenodo (2025), https://doi.org/10.5281/zenodo.14892898.